

Frequency-Modulated Visual Restoration for Matryoshka Large Multimodal Models

Qingtao Pan¹ Zhihao Dou¹ Shuo Li^{1*}

¹Case Western Reserve University

Abstract

Large Multimodal Models (LMMs) struggle to adapt varying computational budgets due to numerous visual tokens. Previous methods attempted to reduce the number of visual tokens before or within LLMs. However, these strategies inevitably result in the loss of visual semantic. To address these issues, we introduce **FMVR**, a plug-and-play and extremely simple **F**requency-**M**odulated **V**isual **R**estoration strategy to boost the reasoning ability of LMMs under visual token reduction. Specifically, FMVR disentangles the visual representation of fewer visual tokens into low- and high-frequency components through AvgPool and MaxPool. The derived frequencies are subsequently modulated using lightweight learnable parameters. The high-frequency from AvgPool acts as a saliency filter to enhance saliency visual semantics, while the low-frequency from MaxPool acts as an anti-saliency filter to strengthen weak visual semantics. It enables the preservation of visual semantics dominated by few visual tokens and the restoration of diluted visual semantics. Additionally, we inject FMVR into Matryoshka Representation Learning to learn coarse-to-fine visual token sets, thus enabling to elastically adjust the number of visual tokens during inference while maintaining comparable performance. Experiments across 10 image-based and 4 video-based bench marks demonstrate that FMVR-LLaVA reduce the FLOPs of LLaVA-1.5-7B by 89%, while maintaining almost 100% of the original accuracy. The code will be open.

1. Introduction

Empowered by the linguistic reasoning capacity of large language models (LLMs) [3, 7, 66, 71], Large Multimodal Models (LMMs) [14, 35, 45, 67] extend the reasoning capabilities of LLMs to the visual domain, achieving joint understanding across visual and linguistic modalities. These LMMs typically utilize a visual encoder to transform im-

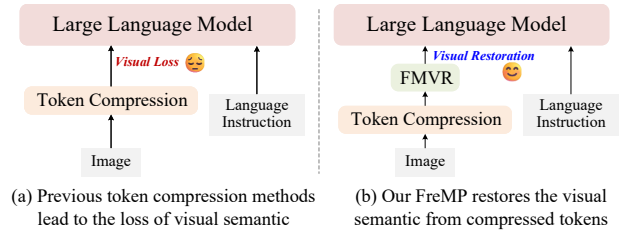


Figure 1. Our FMVR (b) can restore the visual semantics from compressed tokens, alleviating the loss of visual contents in previous token compression methods (a).

ages into discrete visual tokens, which are subsequently fused with textual tokens and processed by a large language model backbone.

In practice, the token budget available to different applications can vary considerably depending on computational constraints and real-time performance requirements. In resource-limited scenarios, a smaller token capacity is often mandated to maintain processing efficiency. Nevertheless, most LMMs employ relatively high visual token count per image. Given that both computational time and memory consumption increase quadratically with the input sequence length [16, 21, 30, 65, 85], using a large number of visual tokens can significantly exacerbate the computational overhead of LMMs. Moreover, in video [42, 78, 84] or high-resolution scenarios [24, 48, 53], the number of required visual tokens can increase dramatically. Consequently, excessive tokenization not only slows inference but also, due to the lack of adaptive visual token allocation at deployment time, restricts the scalability and flexibility of LMMs in practical applications [73].

To alleviate this issue, prior studies [8, 13, 60, 75] have turned to visual token compression, aiming to discard redundant visual tokens while preserving essential semantic information. Despite their effectiveness, these methods inherently yield outputs with a fixed sequence length, without flexibility to adjust the number of visual tokens. Such rigidity hinders the ability to dynamically balance the trade-off between visual tokens and computational cost, which is par-

*Corresponding author: shuo.li11@case.edu



Figure 2. Grad-CAM visualization (576 and 36 visual tokens) shows that the reduction of visual tokens leads to a noticeable degradation in visual focus.

ticularly crucial for computational limitations. Inspired by Matryoshka Representation Learning [34], several studies [6, 26] have investigated training a unified model capable of processing variable numbers of visual tokens (Fig. 1(a)), enabling it to adapt dynamically to different input granularities and computational budgets. However, these methods lead to semantic loss for detailed images, which hampers the model’s ability to capture subtle visual content, leading to poor image understanding performance.

To further substantiate this, we performed a preliminary experiment analyzing the impact of reduced visual tokens on imaging understanding. As shown in Fig. 2, the Grad-CAM reveals a noticeable degradation in visual contents when the number of visual tokens is reduced (576→36). In contrast, a full set of visual tokens (576) exhibits dense visual attention, focusing on nuanced visual regions. This observation highlights the importance of preserving detailed visual contents under token reduction.

Motivated by the above observation, we seek to tackle a pivotal issue: *How to enhance LMM’s reasoning capability under limited visual token budgets.* To achieve this, inspired by the frequency components in feature restoration [18], we propose FMVR, a **F**requency-**M**odulated **V**isual **R**estoration strategy that recovers visual semantics from compressed visual tokens. Concretely, FMVR can disentangle the visual representation into distinct low- and high-frequency components through AvgPool and MaxPool. These frequency components are then refined through lightweight and learnable modulation parameters. The high-frequency from AvgPool acts as a saliency filter to enhance saliency visual semantics, while the low-frequency from MaxPool act as an anti-saliency filter to strengthen weak visual semantics. Subsequently, we inject FMVR into

Matryoshka Representation Learning (MRL) to construct nested visual tokens for LMM training, enabling LMM to elastically adjust visual tokens according to computational constraints while retaining effective reasoning ability. We summarize our contributions as follows:

- We conduct an analysis of the phenomenon where visual token reduction impairs the model’s ability to focus nuanced visual semantics.
- The idea of visual restoration in token compressed LMM is first formulated to alleviate visual semantic degradation induced by token sparsity.
- FMVR, a plug-and-play and extremely simple visual token semantic restoration method, is proposed to highlight diluted visual semantics by disentangling and modulating the frequency components derived from limited visual tokens, thus enriching visual representations.
- Combining FMVR and Matryoshka Representation Learning, it achieves elastically and efficient visual reasoning across varying computational budgets.
- FMVR-LLaVA consistently outperforms prior state-of-the-art methods in various image and video understanding benchmarks, while exploring the trade-off between the accuracy and the number of visual tokens.

2. Related work

Large Multimodal Models. The advancements in Large Language Models (LLMs) [3, 7, 29, 66, 71, 86] have catalyzed a paradigm shift in artificial intelligence, inspiring researchers to extend linguistic reasoning to the multimodal domain, including image understanding [36, 51, 61] and medical imaging [56, 57]. In such models, visual inputs are discretized into token representations to fully leverage the inference capabilities of LLMs. However, visual token representations are dense and spatially redundant, resulting in a significant token expansion. For instance, LLaVA-1.5 [45] transforms a 336×336 image into 576 tokens. Therefore, improving inference efficiency has emerged as a pivotal factor for the scalability and practical deployment of LMMs.

Visual Token Reduction. To achieve compact visual representations, a variety of approaches have been proposed to reduce the number of visual tokens while retaining essential semantic information. Early studies [20, 22, 38, 79, 87] primarily relied on the Q-Former [38], which transforms visual embeddings into a set of fixed-length learnable queries. Although these approaches help alleviate performance degradation induced by token compression, they remain constrained by a prespecified pruning threshold. Recent methods [6, 26], inspired by Matryoshka Representation Learning [34], introduce a hierarchical nesting mechanism for visual tokens, enabling models to represent visual information at multiple granularities. However, these methods inevitably cause information degradation, thereby impair-

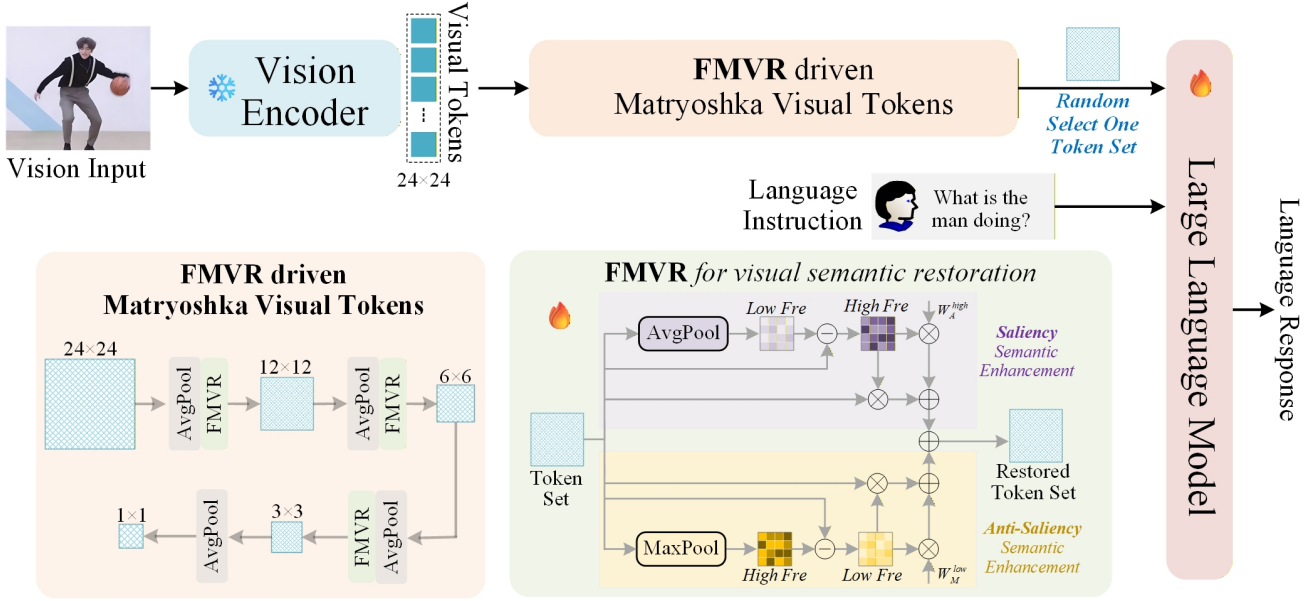


Figure 3. **Illustration of FMVR-LLaVA.** The FMVR is injected into MRL to construct nested visual tokens, where FMVR is used to enhance the visual semantics of each visual token set, thus forming a set of reinforced nested visual tokens for LLM training.

ing the model’s capacity to preserve fine-grained visual semantics when operating with a limited number of visual tokens. The proposed FMVR can alleviate visual information degradation caused by token reduction by decomposing visual representations into low- and high-frequency components, enabling the visual semantic restoration.

3. Method

The FMVR-LLaVA, as illustrated in Fig. 3, proposes a novel visual semantics restoration mechanism, FMVR, to recover nuanced visual contents under compressed visual tokens. By combining the idea of Matryoshka Representation Learning [34], FMVR-LLaVA can support elastically visual token scaling in inference, achieving a favorable balance between computational efficiency and reasoning performance. To be specific, instead of leveraging raw compressed visual tokens, FMVR decomposes the compressed visual representations into low- and high-frequency components to highlight diluted visual semantics.

3.1. Preliminaries

Problem Formulation. Typically, LMMs comprise three core components: vision encoder f_V , modality projector f_M , and LLM f_{LLM} . For simplicity, we define that visual features $H^V = f_M(f_V(X^V)) \in \mathbb{R}^{M \times d}$, where X^V is the input image, M denotes the length of vision tokens, and d is the hidden dimension size; textual features $H^T \in \mathbb{R}^{N \times d}$ where N denotes length of text tokens. In practice, M is generally much larger than N . The LLM utilizes the visual

and textual features to generate output responses X^R . However, the excessive number of visual tokens significantly increases computational cost, resulting in inefficient inference [13]. Hence, vision token compression can effectively reduce M could ameliorate this inefficiency.

Matryoshka Representation Learning (MRL). MRL is designed to jointly optimize embeddings across multiple dimensional scales. Let E denote the set of target embedding dimensions. MRL introduces a learnable model for each subset $v_{1:e} \in \mathbb{R}^e$, where $e \in E$. This strategy allows each truncated representation to be independently optimized under the shared objective. The formal objective function of MRL is defined as:

$$\mathcal{L}_{MRL} = \sum_{e \in E} c_e \mathcal{L} \left(\mathbf{W}^{(e)} \cdot f(x; \theta_f)_{1:e}; y \right), \quad (1)$$

where \mathcal{L} refers to the objective loss and y the ground-truth label. During optimization, MRL simultaneously performs forward and backward updates across all E submodels. Once trained, it enables inference with any embedding size $d \leq E$, achieving scalable deployment depending on resource constraints. Building on this concept, we aim to extend it to LMMs that can dynamically adjust visual tokens for elastic multimodal reasoning.

3.2. FMVR driven Matryoshka Visual Tokens

Matryoshka-style nested visual tokens is constructed by progressively performing 2×2 pooling with a stride of 2. To be specific, the CLIP visual encoder [58] processes an input image X^V as 24×24 visual tokens. Such 24×24 visual

tokens are gradually pooled into 12×12, 6×6, 3×3, and 1×1 visual tokens, thus constructing S nested visual tokens (i.e., $S_i \in \{1, 9, 36, 144, 576\}$), where fewer tokens are obtained by progressively compressing denser tokens. To enhance the visual semantics of each visual token set, we propose FMVR and inject it into each 2×2 pooling operation.

3.3. FMVR for visual semantic restoration

Visual token compression in LMMs tends to the loss of visual information, which is essential for visual understanding. To mitigate this, we introduce FMVR, which highlights subtle visual semantics by disentangling and modulating the frequency components derived reduced visual tokens. As shown in Fig. 3, FMVR contains two distinct pooling units (AvgPool or MaxPool). The AvgPool unit extracts high-frequency to emphasize salient visual semantics. The Max-Pool unit acts as an anti-saliency filter to recover weak visual semantics, avoiding strong salient semantics dominating.

AvgPool Unit for Saliency Semantics Enhancement. To mitigate semantic dilution caused by 2×2 pooling operation in matryoshka visual token construction, we apply AvgPool [17] to extract the low-frequency component X_A^l (captures the global semantic) of each matryoshka visual token set $X \in \mathbb{R}^{C \times H \times W}$. Then we compute the residual between X and X_A^l to obtain the high-frequency component X_A^h , which acts as a saliency filter to highlight saliency visual semantics, calculate as follows:

$$X_A^h = X - X_A^l, \quad X_A^l = \text{AP}(X) \quad (2)$$

where $\text{AP}(\cdot)$ is AvgPool operation. The high-frequency component X_A^h is then modulated by learnable parameters,

$$\hat{X}_A^h = W_A^h \cdot X_A^h, \quad (3)$$

where W_A^h denotes learnable channel-wise parameters that are optimized by backpropagation to select useful frequency subbands. Additionally, the high-frequency is repurposed as attention maps, which are applied multiplicatively to the original input features to boost the activation of visually significant areas. Finally, the high-frequency component and attention weighted features are summed to produce the final representation:

$$\hat{X}_A = \hat{X}_A^h + X_A^h \cdot X \quad (4)$$

However, when a strongly salient semantic dominates the visual representation, weaker semantics are likely to remain overshadowed.

MaxPool Unit for Anti-saliency Semantics Enhancement. To address the dominance of over-salient semantics, the MaxPool is utilized for weaker visual semantics (i.e., anti-saliency Semantics) enhancement. Specifically,

we first extract high-frequency component X_M^h that represents relatively significant semantics through MaxPool. Then we compute the residual between X and X_M^h to capture the differences between non-salient and salient semantics. Intuitively, this residual denotes the low-frequency X_M^l , which acts as an anti-saliency filter that suppresses the dominant semantics and explicitly enhances the latent weak semantics.

$$X_M^l = X - X_M^h, \quad X_M^h = \text{MP}(X), \quad (5)$$

where $\text{MP}(\cdot)$ is MaxPool operation. Similarly, the low-frequency X_M^l is also modulated using learnable parameters:

$$\hat{X}_M^l = W_M^l \cdot X_M^l, \quad (6)$$

where W_M^l is learnable modulation parameters. The low-frequency is employed as attention maps to reactivate suppressed semantics. The output of MaxPool Unit is,

$$\hat{X}_M = \hat{X}_M^l + X_M^l \cdot X \quad (7)$$

The final restored token set is the sum of \hat{X}_A and \hat{X}_M .

4. Experiments

4.1. Experimental Setup

Implementation Details. We implement our models based on LLaVA-1.5 [46] and LLaVA-NeXT [48]. They leveraging Vicuna-7B as base language model. Following [46], we employ a two-stage training paradigm. In the first-stage, we train only the FMVR on LLaVA-558K for one epoch with a batch size of 256 and a learning rate of 1e-3. In the second-stage, for LLaVA-1.5, we finetune FMVR and LLM using LLaVA-665K with a learning rate of LLM of 2e-5 for LLM; for LLaVA-NeXT, we finetune FMVR and LLM using LLaVA-1M [11] with a learning rate of LLM of 1e-5. For both models, the visual encoder is optimized with a learning rate of 2e-5. Both models are trained for one epoch on 4 NVIDIA H100 GPUs.

Evaluation benchmarks. We evaluate our method across 10 image-based benchmarks, including VQAv2 [23], GQA [27], VizWiz [25], ScienceQA-IMG [52], POPE [40], MME [9], MMBench [50], MMBench-CN [50], MMVet [76], and TextVQA [62]. We also conduct experiments on 4 video understanding benchmarks, including MSVD-QA [10], MSRVT-QA [70], ActivityNet-QA [5], and video-based generative performance benchmark [54].

4.2. FMVR for Image Understanding

Our FMVR-LLaVA achieves comparable results on 10 mainstream multimodal understanding and reasoning benchmarks. Table 1 presents the performance of different LMMs and token pruning methods. Among the average performance of 10 benchmarks, FMVR-LLaVA with only

Table 1. Performance comparison on LLaVA-1.5-7B across 10 image-based benchmarks. ‘#VisionTokens’ is the number of vision tokens. Δ rows show the change vs. LLaVA baseline.

Methods	#Vision Tokens	VQAv2	GQA	VisWiz	SQA ^{IMG}	VQA ^{Text}	POPE	MME	MMB ^{EN}	MMB ^{CN}	MMVet	Avg. (%)
BLIP-2 [37]	32	65.0	41.0	19.6	61.0	42.5	85.3	1293.8	31.2	–	22.4	–
InstructBLIP [19]	32	72.4	49.2	34.5	60.5	50.1	86.1	1391.4	36.0	23.7	26.2	50.8
IDEFICS-9B [28]	64	50.9	38.4	35.5	53.5	25.9	81.9	1177.3	48.2	–	30.0	–
IDEFICS-80B [28]	64	60.0	45.2	36.0	61.8	30.9	66.0	1518.2	54.5	–	39.7	–
Qwen-VL [4]	256	78.8	59.3	35.2	67.1	63.8	70.0	1487.6	38.2	7.4	13.0	50.7
Qwen-VL-Chat [4]	256	78.2	57.5	38.9	68.2	60.7	74.9	1487.5	60.6	–	47.3	–
SPHINX [44]	289	78.1	62.6	39.9	69.3	51.6	80.7	1476.1	66.9	–	36.0	–
mPLUG-OwL2 [74]	1024	79.4	56.1	54.5	68.7	54.3	84.6	1450.2	64.5	–	36.2	–
LLaVA-v1.5 [45]	576	78.5	62.0	50.0	66.8	58.2	85.9	1510.7	64.3	58.3	30.5	63.0
LLMs with vision token reduction methods												
FastV [12]	192	67.1	52.7	46.7	65.2	52.5	64.8	1312.4	61.2	55.4	27.7	55.9
PyramidDrop [69]	192	76.1	57.1	51.3	70.2	56.1	82.3	1462.3	63.2	56.3	30.5	61.6
SparseVLM [83]	192	75.6	57.6	51.6	67.2	56.1	83.6	1382.8	62.5	56.7	31.5	61.2
Prumerge+ [60]	144	76.8	59.3	49.8	68.3	57.1	84.0	1462.4	64.9	53.2	30.1	61.7
TRIM [63]	128	75.4	58.4	51.6	68.6	52.2	85.3	1413.4	63.0	52.3	29.9	60.7
VisionZip [72]	192	76.8	59.3	51.2	68.9	57.3	85.3	1469.3	63.0	57.0	31.7	62.4
DART [68]	128	74.7	57.9	52.8	69.1	56.3	80.4	1408.7	60.7	57.3	30.9	61.1
DivPrune [1]	128	76.0	59.4	52.8	68.6	55.9	87.0	1405.1	61.5	54.8	30.6	61.7
CDPruner [81]	128	76.6	59.9	52.8	69.0	56.2	87.7	1431.4	63.1	55.0	32.8	62.5
VisPruner [80]	128	75.8	58.2	52.7	69.1	57.0	84.6	1461.4	62.7	57.3	33.7	62.4
MQT-LLaVA [26]	144	76.4	61.4	52.0	67.5	53.4	83.9	1446.4	64.4	57.2	29.9	61.8
M3 [6]	144	78.5	61.3	53.1	65.2	54.8	87.0	1451.5	66.4	56.3	30.2	62.5
Ours												
FMVR-LLaVA	1	68.3	55.2	49.7	68.6	49.2	81.1	1284.8	60.7	53.4	26.4	57.7
	9	74.5	59.1	50.7	69.9	50.8	84.1	1415.0	64.2	57.5	29.0	61.1
	36	76.5	60.9	52.9	69.5	55.3	85.9	1452.5	65.2	58.3	32.2	62.9
	144	78.6	62.3	55.1	69.7	55.5	86.4	1473.9	65.8	57.6	33.4	63.8
	576	79.2	63.0	56.5	68.9	57.8	87.5	1510.1	65.9	58.0	34.3	64.7
Δ vs. LLaVA-v1.5	144	+0.1	+0.3	+5.1	+2.9	-2.7	+0.5	-36.8	+1.5	-0.7	+2.9	+0.8

Table 2. Ablation study of applying different pooling unit in FMVR.

Method	VQAv2	GQA	VisWiz	SQA ^{IMG}	VQA ^{Text}	POPE	MME	MMB ^{EN}	MMB ^{CN}	MMVet	Avg. (%)
M3 (Baseline)	78.5	61.3	53.1	65.2	54.8	87.0	1451.5	66.4	56.3	30.2	62.5
FMVR (Ours)	78.6	62.3	55.1	69.7	55.5	86.4	1473.9	65.8	57.6	33.4	63.8
FMVR w/o AvgPool	77.9	62.0	54.6	68.1	54.3	85.7	1459.6	65.4	56.7	32.5	63.0
FMVR w/o MaxPool	78.3	62.6	53.3	68.4	55.0	86.9	1463.7	65.8	57.1	32.6	63.3

144 visual tokens outperforms LLaVA-1.5 with 576 visual tokens by 0.8%. Additionally, when retaining only 36 visual tokens, our method surpasses all the LLMs with vision token reduction methods in Table 1. Notably, when drastically drop to only 1 token, our method still outperform FastV, InstructBLIP, and Qwen-VL by 1.8%, 6.9%, and 7.0%, respectively. Our method also consistently outperforms MRL based methods, as shown in Fig. 4, under different numbers of visual tokens, our method exceeds both M3 and MQT-

LLaVA on MMVet, SQA, GQA, and POPE. This means that our method can effectively improve visual semantics in the case of reduced visual tokens.

4.3. FMVR for high-Resolution Understanding

Increasing the resolution of input images generally enhances the reasoning capacity of LLMs. However, this gain comes at the cost of significantly higher computational complexity. For a fair comparison, we standardize

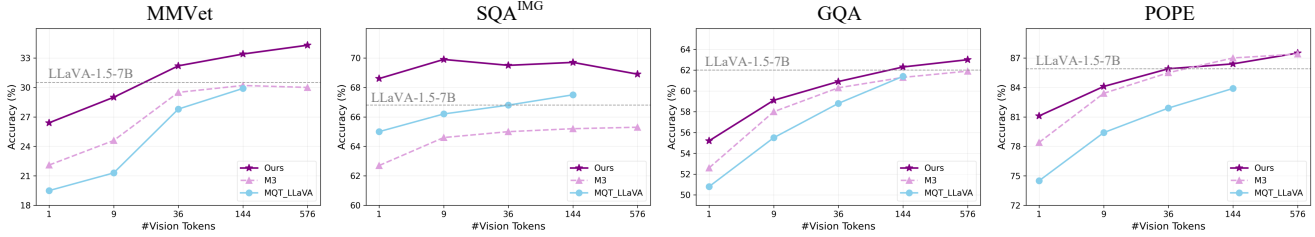


Figure 4. Comparison under different numbers of vision tokens. Our method achieves higher accuracy than M3 and MQT-LLaVA.

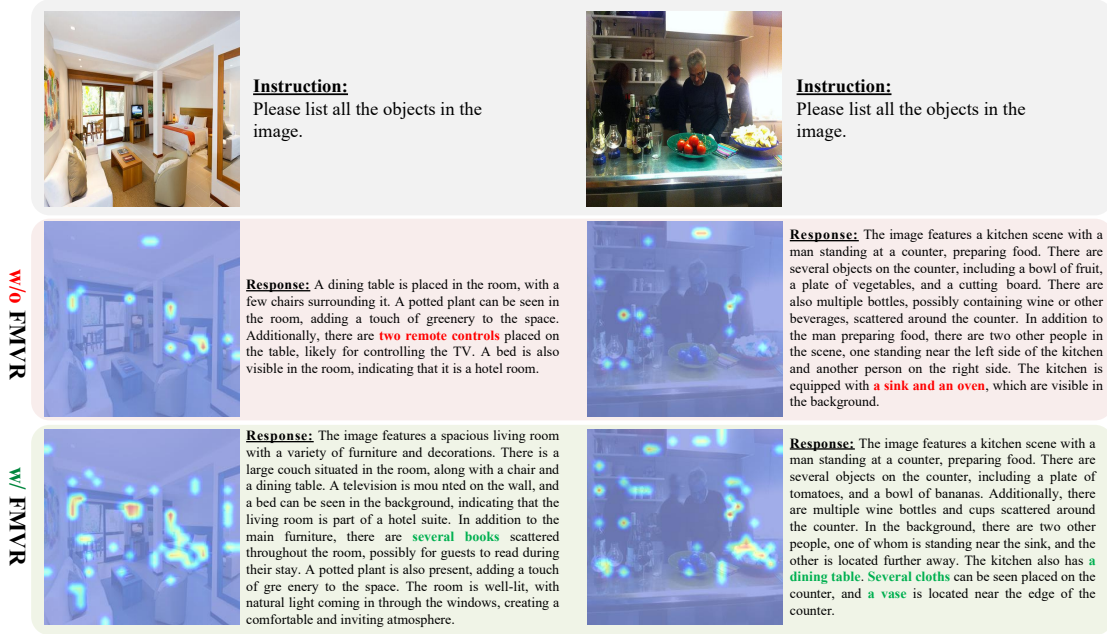


Figure 5. Grad-CAM visualization and response comparison between w/o FMVR and w FMVR under 36 visual tokens. From Grad-CAM visualization, the reduction of visual tokens leads to a noticeable degradation in visual semantics, which leads to hallucinations of certain objects in the response.

Table 3. Efficiency analysis of different numbers of vision tokens on LLaVA-1.5-7B.

Methods	Tokens	FLOPs (TB)	Prefill Time (ms)	Total Memory (GB)	Avg (%)
LLaVA-v1.5	576	8.0	58.1	21.6	63.0
FMVR	144	2.2 (×3.6)	19.5 (×3.0)	15.0 (×1.4)	63.8
	36	0.9 (×8.9)	18.0 (×3.2)	13.8 (×1.6)	62.9
	9	0.5 (×16)	17.7 (×3.3)	13.6 (×1.6)	61.1
	1	0.4 (×20)	17.6 (×3.3)	13.5 (×1.6)	57.7

the input resolution to 672×672, corresponding to 2,880 visual tokens. Table 6 shows the performance comparison

Table 4. FLOPs of each component in FMVR-LLaVA.

Methods	Vision Encoder	Projection	FMVR	LLM	Total
LLaVA-v1.5	0.349	0.024	-	8.0	8.37
FMVR ⁵⁷⁶	0.349	0.024	6.4e-5	8.0	8.37

Table 5. Efficiency analysis of different pruning methods on LLaVA-1.5-7B.

Methods	Tokens	FLOPs (TB)	Prefill Time (ms)	Avg (%)
FastV	192	2.1	34.1	55.9
PDrop	192	2.0	36.7	61.6
SparseVLM	192	2.1	36.5	61.2
FMVR	36	0.9	18.0	62.9

Table 6. Performance comparison on LLaVA-NeXT-7B across 10 image-based benchmarks. ‘#VisionTokens’ is the number of vision tokens. Δ rows show the change vs. LLaVA-NeXT-7B baseline.

Methods	#Vision Tokens	VQAv2	GQA	VisWiz	SQA ^{IMG}	VQA ^{Text}	POPE	MME	MMB ^{EN}	MMB ^{CN}	MMVet	Avg. (%)
LLaVA-NeXT-7B [47]	2880	81.3	62.5	55.2	67.5	60.3	86.8	1511.8	65.8	57.3	40.0	65.2
FastV [12]	320	61.5	49.8	51.3	66.6	52.2	49.5	1099.0	53.4	42.5	20.0	50.2
PyramidDrop [69]	320	66.8	50.4	49.7	66.7	49.0	60.8	1171.5	55.5	44.7	24.0	52.6
SparseVLM [83]	320	74.6	57.9	54.2	67.2	56.5	76.9	1386.1	63.1	56.7	32.8	60.9
Prunerge+ [60]	320	75.3	58.8	57.7	68.1	54.0	79.5	1444.3	63.0	55.6	31.4	61.6
TRIM [63]	320	74.9	59.9	53.5	66.2	50.2	86.5	1443.8	63.5	51.0	32.7	61.1
VisionZip [72]	320	76.2	58.9	56.2	67.5	58.8	82.3	1397.1	63.3	55.6	35.8	62.4
DART [68]	320	75.7	59.5	56.8	67.5	57.6	81.0	1419.5	64.2	55.7	35.7	62.5
DivPrune [1]	320	77.2	61.1	55.6	67.7	56.2	84.7	1423.3	63.9	55.7	34.8	62.8
CDPruner [81]	320	78.4	61.6	55.8	67.8	57.4	87.2	1453.0	65.5	55.7	37.9	64.0
VisPruner [80]	320	75.7	58.4	–	–	57.6	80.4	1370.1	–	–	–	–
M3 [6]	180	–	–	–	72.1	58.7	87.3	–	68.6	–	–	–
Ours												
FMVR-LLaVA	5	71.4	54.3	49.7	64.6	53.2	81.7	1365.4	62.3	52.8	29.4	58.8
	45	74.1	57.3	52.4	66.8	56.4	84.6	1422.5	61.9	53.1	34.0	61.2
	180	78.2	61.4	55.3	68.6	58.3	87.6	1456.8	65.9	56.3	37.5	64.2
	720	79.4	62.5	57.4	70.3	58.0	87.3	1487.6	66.5	57.1	36.9	65.0
	2880	82.4	62.1	56.3	70.6	59.2	88.0	1526.7	67.1	56.9	38.2	65.7

Table 7. Performance comparison on LLaVA-NeXT-7B across 4 video-based benchmarks. ‘#VisionTokens’ is the number of vision tokens. Δ rows show the change vs. LLaVA-NeXT-7B baseline.

Methods	#Vision Tokens	Video-based Question-Answer				Video-based Generative Performance					
		MSVD	MSRVTT	ActivityNet	Avg.	Correct.	Detail	Context.	Temp.	Consist.	Avg.
LLaMA Adapter [82]	1280	54.9	43.8	34.2	44.3	2.03	2.32	2.30	1.98	2.15	2.16
VideoChat [39]	512	56.3	45.0	26.5	42.6	2.23	2.50	2.53	1.94	2.24	2.29
Video-LLAMA [77]	1024	51.6	29.6	12.4	31.2	1.96	2.18	2.16	1.82	1.79	1.98
Video-ChatGPT [39]	~360	64.9	49.3	35.2	49.8	2.40	2.52	2.62	1.98	2.37	2.38
BT-Adapter [49]	~260	67.5	57.0	45.7	56.7	2.68	2.69	3.27	2.34	2.46	2.69
MovieChat [64]	65536	75.2	52.7	45.7	57.9	2.76	2.93	3.01	2.24	2.42	2.67
LLaMA-VID [41]	1fpsx2	69.7	57.7	47.4	58.3	2.96	3.00	3.53	2.46	2.51	2.89
Video-LLaVA [42]	2048	70.7	59.2	45.3	58.4	2.87	2.94	3.44	2.45	2.51	2.84
FastV [12]	198	38.0	19.3	30.6	29.3	–	–	–	–	–	–
SparseVLM [83]	198	68.2	31.0	42.6	47.3	–	–	–	–	–	–
VisionZip [72]	136	63.5	52.1	43.0	52.9	–	–	–	–	–	–
VisPruner [80]	227	69.3	55.6	–	–	–	–	–	–	–	–
Ours											
FMVR-LLaVA	5	68.7	52.4	45.1	55.4	2.54	2.77	2.83	2.34	2.41	2.58
	45	74.2	58.3	49.6	60.7	2.91	2.88	3.23	2.41	2.46	2.78
	180	76.9	62.5	51.1	63.5	3.30	3.55	3.72	2.84	3.10	3.30
	720	78.7	64.8	53.5	65.7	3.45	3.62	3.77	3.05	3.21	3.42
	2880	79.1	65.2	53.4	65.9	3.49	3.71	3.85	3.14	3.44	3.53
Δ vs. Video-LLaVA	180	+6.2	+3.3	+5.8	+5.1	+0.43	+0.61	+0.28	+0.39	+0.59	+0.46

on LLaVA-NeXT-7B across 10 image-based benchmarks. Our FMVR-LLaVA (720 visual tokens) achieves comparable performance compared to LLaVA-NeXT-7B (2880 visual tokens), i.e., 65.0% vs. 65.2%. Even under only 180 vi-

sual tokens, FMVR-LLaVA outperforms all the visual token reduction methods, respectively. Notably, FMVR-LLaVA with only 5 visual tokens significantly exceeds FastV and PyramidDrop by 8.6% and 6.2%, respectively. These find-

ings demonstrate FMVR-LLaVA’s remarkable efficiency in high-resolution multimodal reasoning scenarios.

4.4. FMVR for video Understanding

We compare FMVR-LLaVA against state-of-the-art video LLMs across 4 video benchmarks. Following IG-VLM [32], LLaVA-NeXT-7B based FMVR-LLaVA is directly used for video reasoning. For our method, 5 frames are uniformly sampled over the entire video. As shown in Table 7, with only 180 visual tokens, our method outperforms Video-LLaVA by 5.1% on Video-based Question-Answer and 0.46% on Video-based Generative Performance, respectively. These results further demonstrate the effectiveness of FMVR-LLaVA in video understanding.

4.5. Efficiency analysis

To demonstrate the efficiency of FMVR-LLaVA, we conduct efficiency analysis of different numbers of vision tokens on LLaVA-1.5-7B, FLOPs of each component in FMVR-LLaVA, and efficiency analysis of different pruning methods on LLaVA-1.5-7B. As shown in Table 3, our method with 36 visual tokens achieves a $\times 8.9$ FLOPs reduction compared to LLaVA-v1.5 while maintaining almost same performance. To further study computational load of each component, we compute the FLOPs of each module (Table 4). The computational cost (with only $6.4e-5$) of the proposed FMVR is negligible. The comparative analysis against other pruning methods shows that our method gains the best efficiency while maintaining the highest performance. Compared to FastV, our method achieves nearly a $\times 2.3$ reduction in FLOPs and a $\times 1.9$ reduction in Prefill time, while outperforming FastV by 7.0%.

4.6. Ablation Study

We further conduct an ablation on the design of FMVR-LLaVA. For simplicity, we evaluate all the models with 144 visual tokens. As shown in Table 2, FMVR without Max-Pool unit results in performance degradation by 0.5% due to the loss of edge feature enhancement. Similarly, the absence of AvgPool unit also lead to a 0.8% performance degradation. In addition, compared to the baseline M3, both AvgPool and MaxPool bring performance improvements, demonstrating their importance of restoring visual semantics with reduced visual tokens.

4.7. Case Study and Visualization Analysis

Fig. 6 presents examples of FMVR-LLaVA in image understanding tasks. Despite using only one visual token, our method can provide the correct answer. However, for slightly complex images, such as the third case, the answer using only one visual token is incorrect. Fortunately, increasing the number of visual tokens slightly (i.e., 9 visual tokens) can provide the correct answer. To further explore

the effectiveness of FMVR, we utilize Grad-CAM [59] to visualize the focus of visual information using 36 visual tokens. From Grad-CAM visualization results, we can see that the reduction of visual tokens leads to a noticeable degradation in visual semantics, which leads to hallucinations of certain objects in the response. On the contrary, when applying FMVR, the focus on visual semantics increases, leading to more accurate responses.

5. Conclusion

In this paper, we propose FMVR, a novel visual token semantic restoration method, to enhance the efficiency of LLMs under token reduction. By disentangling visual representations into low- and high-frequency components, FMVR enables the preservation of visual semantics dominated by few visual tokens and the restoration of diluted visual semantics. By integrating FMVR into MRL, it can dynamically adjust the number of visual tokens during inference while maintaining comparable performance. Extensive experiments across 10 image and 4 video benchmarks validate the effectiveness of FMVR under token reduction.

References

- [1] Saeed Ranjbar Alvar, Gursimran Singh, Mohammad Akbari, and Yong Zhang. Divprune: Diversity-based visual token pruning for large multimodal models. In *Proceedings of the Computer Vision and Pattern Recognition Conference*, pages 9392–9401, 2025. 5, 7, 15
- [2] Stanislaw Antol, Aishwarya Agrawal, Jiasen Lu, Margaret Mitchell, Dhruv Batra, C Lawrence Zitnick, and Devi Parikh. Vqa: Visual question answering. In *Proceedings of the IEEE international conference on computer vision*, pages 2425–2433, 2015. 13
- [3] Jinze Bai, Shuai Bai, Yunfei Chu, Zeyu Cui, Kai Dang, Xiaodong Deng, Yang Fan, Wenbin Ge, Yu Han, Fei Huang, et al. Qwen technical report. *arXiv preprint arXiv:2309.16609*, 2023. 1, 2, 13
- [4] Jinze Bai, Shuai Bai, Shusheng Yang, Shijie Wang, Sinan Tan, Peng Wang, Junyang Lin, Chang Zhou, and Jingren Zhou. Qwen-vl: A frontier large vision-language model with versatile abilities. *arXiv preprint arXiv:2308.12966*, 2023. 5
- [5] Fabian Caba Heilbron, Victor Escorcia, Bernard Ghanem, and Juan Carlos Niebles. Activitynet: A large-scale video benchmark for human activity understanding. In *Proceedings of the IEEE conference on computer vision and pattern recognition*, pages 961–970, 2015. 4, 14
- [6] Mu Cai, Jianwei Yang, Jianfeng Gao, and Yong Jae Lee. Matryoshka multimodal models. *arXiv preprint arXiv:2405.17430*, 2024. 2, 5, 7, 15
- [7] Zheng Cai, Maosong Cao, Haojiong Chen, Kai Chen, Keyu Chen, Xin Chen, Xun Chen, Zehui Chen, Zhi Chen, Pei Chu, et al. Internlm2 technical report. *arXiv preprint arXiv:2403.17297*, 2024. 1, 2
- [8] Junbum Cha, Wooyoung Kang, Jonghwan Mun, and Byungseok Roh. Honeybee: Locality-enhanced projector

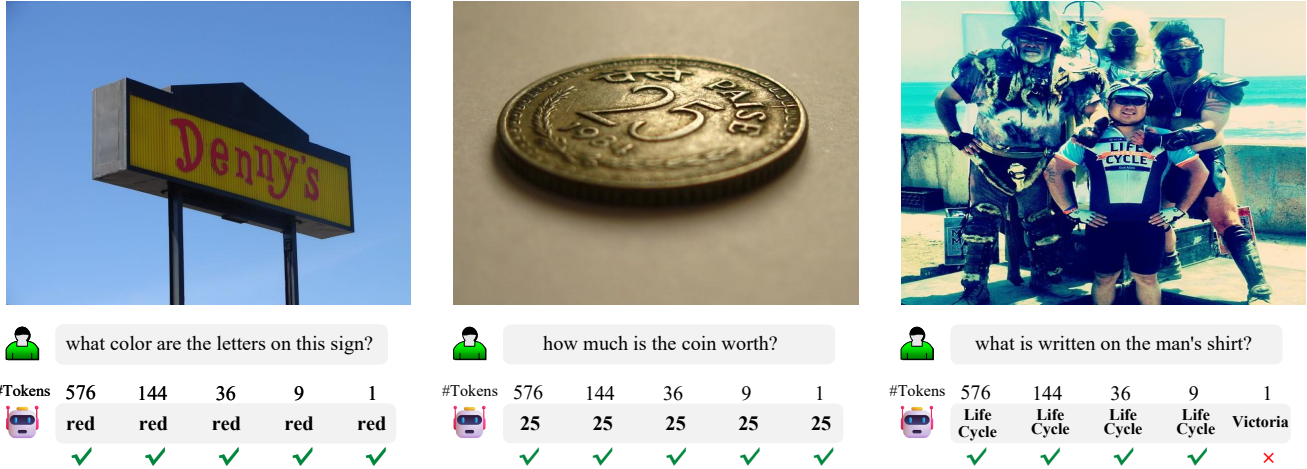


Figure 6. Case of image understanding on different VQA prompts. Our method yields basically correct answers under different numbers of visual tokens.

for multimodal llm. In *Proceedings of the IEEE/CVF Conference on Computer Vision and Pattern Recognition*, pages 13817–13827, 2024. 1

- [9] Fu Chaoyou, Chen Peixian, Shen Yunhang, Qin Yulei, Zhang Mengdan, Lin Xu, Yang Jinrui, Zheng Xiawu, Li Ke, Sun Xing, et al. Mme: A comprehensive evaluation benchmark for multimodal large language models. *arXiv preprint arXiv:2306.13394*, 2023. 4, 14
- [10] David Chen and William B Dolan. Collecting highly parallel data for paraphrase evaluation. In *Proceedings of the 49th annual meeting of the association for computational linguistics: human language technologies*, pages 190–200, 2011. 4, 14
- [11] Lin Chen and Long Xing. Open-llava-next: An open-source implementation of llava-next series for facilitating the large multi-modal model community. 2024. 4
- [12] Liang Chen, Haozhe Zhao, Tianyu Liu, Shuai Bai, Junyang Lin, Chang Zhou, and Baobao Chang. An image is worth 1/2 tokens after layer 2: Plug-and-play inference acceleration for large vision-language models. In *European Conference on Computer Vision*, pages 19–35. Springer, 2024. 5, 7, 15
- [13] Liang Chen, Haozhe Zhao, Tianyu Liu, Shuai Bai, Junyang Lin, Chang Zhou, and Baobao Chang. An image is worth 1/2 tokens after layer 2: Plug-and-play inference acceleration for large vision-language models. In *European Conference on Computer Vision*, pages 19–35. Springer, 2024. 1, 3
- [14] Zhe Chen, Jiannan Wu, Wenhai Wang, Weijie Su, Guo Chen, Sen Xing, Muyan Zhong, Qinglong Zhang, Xizhou Zhu, Lewei Lu, et al. Internvl: Scaling up vision foundation models and aligning for generic visual-linguistic tasks. In *Proceedings of the IEEE/CVF conference on computer vision and pattern recognition*, pages 24185–24198, 2024. 1
- [15] Wei-Lin Chiang, Zhuohan Li, Ziqing Lin, Ying Sheng, Zhanghao Wu, Hao Zhang, Lianmin Zheng, Siyuan Zhuang, Yonghao Zhuang, Joseph E Gonzalez, et al. Vicuna: An open-source chatbot impressing gpt-4 with 90%* chatgpt quality. See <https://vicuna.lmsys.org> (accessed 14 April 2023), 2(3):6, 2023. 13
- [16] Krzysztof Choromanski, Valerii Likhoshesterov, David Doan, Xingyou Song, Andreea Gane, Tamas Sarlos, Peter Hawkins, Jared Davis, Afroz Mohiuddin, Lukasz Kaiser, et al. Rethinking attention with performers. *arXiv preprint arXiv:2009.14794*, 2020. 1
- [17] Yuning Cui, Yi Tao, Zhenshan Bing, Wenqi Ren, Xinwei Gao, Xiaochun Cao, Kai Huang, and Alois Knoll. Selective frequency network for image restoration. In *The eleventh international conference on learning representations*. 4
- [18] Yuning Cui, Yi Tao, Zhenshan Bing, Wenqi Ren, Xinwei Gao, Xiaochun Cao, Kai Huang, and Alois Knoll. Selective frequency network for image restoration. In *The eleventh international conference on learning representations*, 2023. 2
- [19] Wenliang Dai, Junnan Li, Dongxu Li, Anthony Tiong, Junqi Zhao, Weisheng Wang, Boyang Li, Pascale N Fung, and Steven Hoi. Instructblip: Towards general-purpose vision-language models with instruction tuning. *Advances in neural information processing systems*, 36:49250–49267, 2023. 5
- [20] Wenliang Dai, Junnan Li, Dongxu Li, Anthony Tiong, Junqi Zhao, Weisheng Wang, Boyang Li, Pascale N Fung, and Steven Hoi. Instructblip: Towards general-purpose vision-language models with instruction tuning. *Advances in neural information processing systems*, 36:49250–49267, 2023. 2
- [21] Tri Dao, Dan Fu, Stefano Ermon, Atri Rudra, and Christopher Ré. Flashattention: Fast and memory-efficient exact attention with io-awareness. *Advances in neural information processing systems*, 35:16344–16359, 2022. 1
- [22] Zhengxiao Du, Yujie Qian, Xiao Liu, Ming Ding, Jiezhong Qiu, Zhilin Yang, and Jie Tang. Glm: General language model pretraining with autoregressive blank infilling. In *Proceedings of the 60th Annual Meeting of the Association for Computational Linguistics (Volume 1: Long Papers)*, pages 320–335, 2022. 2

- [23] Yash Goyal, Tejas Khot, Douglas Summers-Stay, Dhruv Batra, and Devi Parikh. Making the v in vqa matter: Elevating the role of image understanding in visual question answering. In *Proceedings of the IEEE conference on computer vision and pattern recognition*, pages 6904–6913, 2017. 4, 13
- [24] Zonghao Guo, Ruyi Xu, Yuan Yao, Junbo Cui, Zanlin Ni, Chunjiang Ge, Tat-Seng Chua, Zhiyuan Liu, and Gao Huang. Llava-uhd: an lmm perceiving any aspect ratio and high-resolution images. In *European Conference on Computer Vision*, pages 390–406. Springer, 2024. 1
- [25] Danna Gurari, Qing Li, Abigale J Stangl, Anhong Guo, Chi Lin, Kristen Grauman, Jiebo Luo, and Jeffrey P Bigham. Vizwiz grand challenge: Answering visual questions from blind people. In *Proceedings of the IEEE conference on computer vision and pattern recognition*, pages 3608–3617, 2018. 4, 13
- [26] Wenbo Hu, Zi-Yi Dou, Liunian Li, Amita Kamath, Nanyun Peng, and Kai-Wei Chang. Matryoshka query transformer for large vision-language models. *Advances in Neural Information Processing Systems*, 37:50168–50188, 2024. 2, 5, 15
- [27] Drew A Hudson and Christopher D Manning. Gqa: A new dataset for real-world visual reasoning and compositional question answering. In *Proceedings of the IEEE/CVF conference on computer vision and pattern recognition*, pages 6700–6709, 2019. 4, 13
- [28] Introducing IDEFICS. An open reproduction of state-of-the-art visual language model, 2023. 5
- [29] Albert Qiaochu Jiang, Alexandre Sablayrolles, Arthur Mensch, Chris Bamford, Devendra Singh Chaplot, Diego de Las Casas, Florian Bressand, Gianna Lengyel, Guillaume Lample, Lucile Saulnier, L el io Renard Lavaud, Marie-Anne Lachaux, Pierre Stock, Teven Le Scao, Thibaut Lavril, Thomas Wang, Timoth ee Lacroix, and William El Sayed. Mistral 7b. *arXiv preprint arXiv:2310.06825*, 2023. 2
- [30] Angelos Katharopoulos, Apoorv Vyas, Nikolaos Pappas, and Fran ois Fleuret. Transformers are rnns: Fast autoregressive transformers with linear attention. In *International conference on machine learning*, pages 5156–5165. PMLR, 2020. 1
- [31] Aniruddha Kembhavi, Mike Salvato, Eric Kolve, Minjoon Seo, Hannaneh Hajishirzi, and Ali Farhadi. A diagram is worth a dozen images. In *European conference on computer vision*, pages 235–251. Springer, 2016. 14
- [32] Wonkyun Kim, Changin Choi, Wonseok Lee, and Wonjong Rhee. An image grid can be worth a video: Zero-shot video question answering using a vlm. *arXiv preprint arXiv:2403.18406*, 2024. 8
- [33] Ivan Krasin, Tom Duerig, Neil Alldrin, Vittorio Ferrari, Sami Abu-El-Haija, Alina Kuznetsova, Hassan Rom, Jasper Uijlings, Stefan Popov, Andreas Veit, et al. Openimages: A public dataset for large-scale multi-label and multi-class image classification. *Dataset available from <https://github.com/openimages>*, 2(3):18, 2017. 14
- [34] Aditya Kusupati, Gantavya Bhatt, Aniket Rege, Matthew Wallingford, Aditya Sinha, Vivek Ramanujan, William Howard-Snyder, Kaifeng Chen, Sham Kakade, Prateek Jain, et al. Matryoshka representation learning. *Advances in Neural Information Processing Systems*, 35:30233–30249, 2022. 2, 3
- [35] Bo Li, Yuanhan Zhang, Dong Guo, Renrui Zhang, Feng Li, Hao Zhang, Kaichen Zhang, Peiyuan Zhang, Yanwei Li, Ziwei Liu, et al. Llava-onevision: Easy visual task transfer. *arXiv preprint arXiv:2408.03326*, 2024. 1
- [36] Boyi Li, Yifan Shen, Yuanzhe Liu, Yifan Xu, Jiateng Liu, Xinzhuo Li, Zhengyuan Li, Jingyuan Zhu, Yunhan Zhong, Fangzhou Lan, et al. Toward cognitive supersensing in multimodal large language model. *arXiv preprint arXiv:2602.01541*, 2026. 2
- [37] Junnan Li, Dongxu Li, Silvio Savarese, and Steven Hoi. Blip-2: Bootstrapping language-image pre-training with frozen image encoders and large language models. In *International conference on machine learning*, pages 19730–19742. PMLR, 2023. 5
- [38] Junnan Li, Dongxu Li, Silvio Savarese, and Steven Hoi. Blip-2: Bootstrapping language-image pre-training with frozen image encoders and large language models. In *International conference on machine learning*, pages 19730–19742. PMLR, 2023. 2
- [39] KunChang Li, Yanan He, Yi Wang, Yizhuo Li, Wenhai Wang, Ping Luo, Yali Wang, Limin Wang, and Yu Qiao. Videochat: Chat-centric video understanding. *arXiv preprint arXiv:2305.06355*, 2023. 7
- [40] Yifan Li, Yifan Du, Kun Zhou, Jinpeng Wang, Wayne Xin Zhao, and Ji-Rong Wen. Evaluating object hallucination in large vision-language models. In *Proceedings of the 2023 Conference on Empirical Methods in Natural Language Processing*, pages 292–305, 2023. 4, 14
- [41] Yanwei Li, Chengyao Wang, and Jiaya Jia. Llama-vid: An image is worth 2 tokens in large language models. In *European Conference on Computer Vision*, pages 323–340. Springer, 2024. 7
- [42] Bin Lin, Yang Ye, Bin Zhu, Jiayi Cui, Munan Ning, Peng Jin, and Li Yuan. Video-llava: Learning united visual representation by alignment before projection. In *Proceedings of the 2024 Conference on Empirical Methods in Natural Language Processing*, pages 5971–5984, 2024. 1, 7
- [43] Tsung-Yi Lin, Michael Maire, Serge Belongie, James Hays, Pietro Perona, Deva Ramanan, Piotr Doll ar, and C Lawrence Zitnick. Microsoft coco: Common objects in context. In *European conference on computer vision*, pages 740–755. Springer, 2014. 13, 14
- [44] Ziyi Lin, Chris Liu, Renrui Zhang, Peng Gao, Longtian Qiu, Han Xiao, Han Qiu, Chen Lin, Wenqi Shao, Keqin Chen, et al. Sphinx: The joint mixing of weights, tasks, and visual embeddings for multi-modal large language models. *arXiv preprint arXiv:2311.07575*, 2023. 5
- [45] Haotian Liu, Chunyuan Li, Qingyang Wu, and Yong Jae Lee. Visual instruction tuning. *Advances in neural information processing systems*, 36:34892–34916, 2023. 1, 2, 5, 13, 15
- [46] Haotian Liu, Chunyuan Li, Yuheng Li, and Yong Jae Lee. Improved baselines with visual instruction tuning. In *Proceedings of the IEEE/CVF conference on computer vision and pattern recognition*, pages 26296–26306, 2024. 4

- [47] Haotian Liu, Chunyuan Li, Yuheng Li, Bo Li, Yuanhan Zhang, Sheng Shen, and Yong Jae Lee. Llava-next: Improved reasoning, ocr, and world knowledge, january 2024. URL <https://llava-vl.github.io/blog/2024-01-30-llava-next>, 2024. 7, 13
- [48] Haotian Liu, Chunyuan Li, Yuheng Li, Bo Li, Yuanhan Zhang, Sheng Shen, and Yong Jae Lee. Llava-next: Improved reasoning, ocr, and world knowledge, january 2024. URL <https://llava-vl.github.io/blog/2024-01-30-llava-next>, 1(8), 2024. 1, 4
- [49] Ruyang Liu, Chen Li, Yixiao Ge, Thomas H Li, Ying Shan, and Ge Li. Bt-adapter: Video conversation is feasible without video instruction tuning. In *Proceedings of the IEEE/CVF Conference on Computer Vision and Pattern Recognition*, pages 13658–13667, 2024. 7
- [50] Yuan Liu, Haodong Duan, Yuanhan Zhang, Bo Li, Songyang Zhang, Wangbo Zhao, Yike Yuan, Jiaqi Wang, Conghui He, Ziwei Liu, et al. Mmbench: Is your multi-modal model an all-around player? In *European conference on computer vision*, pages 216–233. Springer, 2024. 4, 14
- [51] Yuanzhe Liu, Jingyuan Zhu, Yuchen Mo, Gen Li, Xu Cao, Jin Jin, Yifan Shen, Zhengyuan Li, Tianjiao Yu, Wenzhen Yuan, et al. Palm: Progress-aware policy learning via affordance reasoning for long-horizon robotic manipulation. *arXiv preprint arXiv:2601.07060*, 2026. 2
- [52] Pan Lu, Swaroop Mishra, Tanglin Xia, Liang Qiu, Kai-Wei Chang, Song-Chun Zhu, Oyvind Tafjord, Peter Clark, and Ashwin Kalyan. Learn to explain: Multimodal reasoning via thought chains for science question answering. *Advances in Neural Information Processing Systems*, 35:2507–2521, 2022. 4, 14
- [53] Gen Luo, Yiyi Zhou, Yuxin Zhang, Xiawu Zheng, Xiaoshuai Sun, and Rongrong Ji. Feast your eyes: Mixture-of-resolution adaptation for multimodal large language models. *arXiv preprint arXiv:2403.03003*, 2024. 1
- [54] Muhammad Maaz, Hanoona Rasheed, Salman Khan, and Fahad Khan. Video-chatgpt: Towards detailed video understanding via large vision and language models. In *Proceedings of the 62nd Annual Meeting of the Association for Computational Linguistics (Volume 1: Long Papers)*, pages 12585–12602, 2024. 4, 14
- [55] Ahmed Masry, Xuan Long Do, Jia Qing Tan, Shafiq Joty, and Enamul Hoque. Chartqa: A benchmark for question answering about charts with visual and logical reasoning. In *Findings of the association for computational linguistics: ACL 2022*, pages 2263–2279, 2022. 14
- [56] Qingtao Pan, Zhengrong Li, Guang Yang, Qing Yang, and Bing Ji. Evivlm: When evidential learning meets vision language model for medical image segmentation. *IEEE Transactions on Medical Imaging*, 2025. 2
- [57] Qingtao Pan, Wenhao Qiao, Jingjiao Lou, Bing Ji, and Shuo Li. Duss: dual semantic similarity-supervised vision-language model for semi-supervised medical image segmentation. In *Proceedings of the AAAI Conference on Artificial Intelligence*, pages 6299–6307, 2025. 2
- [58] Alec Radford, Jong Wook Kim, Chris Hallacy, Aditya Ramesh, Gabriel Goh, Sandhini Agarwal, Girish Sastry, Amanda Aspell, Pamela Mishkin, Jack Clark, et al. Learning transferable visual models from natural language supervision. In *International conference on machine learning*, pages 8748–8763. PmlR, 2021. 3, 13
- [59] Ramprasaath R Selvaraju, Michael Cogswell, Abhishek Das, Ramakrishna Vedantam, Devi Parikh, and Dhruv Batra. Grad-cam: Visual explanations from deep networks via gradient-based localization. In *Proceedings of the IEEE international conference on computer vision*, pages 618–626, 2017. 8
- [60] Yuzhang Shang, Mu Cai, Bingxin Xu, Yong Jae Lee, and Yan Yan. Llava-prumerge: Adaptive token reduction for efficient large multimodal models. In *Proceedings of the IEEE/CVF International Conference on Computer Vision*, pages 22857–22867, 2025. 1, 5, 7, 15
- [61] Yifan Shen, Yuanzhe Liu, Jingyuan Zhu, Xu Cao, Xiaofeng Zhang, Yixiao He, Wenming Ye, James Matthew Rehg, and Ismeni Lourentzou. Fine-grained preference optimization improves spatial reasoning in vlms. *arXiv preprint arXiv:2506.21656*, 2025. 2
- [62] Amanpreet Singh, Vivek Natarajan, Meet Shah, Yu Jiang, Xinlei Chen, Dhruv Batra, Devi Parikh, and Marcus Rohrbach. Towards vqa models that can read. In *Proceedings of the IEEE/CVF conference on computer vision and pattern recognition*, pages 8317–8326, 2019. 4, 14
- [63] Dingjie Song, Wenjun Wang, Shunian Chen, Xidong Wang, Michael X Guan, and Benyou Wang. Less is more: A simple yet effective token reduction method for efficient multimodal llms. In *Proceedings of the 31st International Conference on Computational Linguistics*, pages 7614–7623, 2025. 5, 7, 15
- [64] Enxin Song, Wenhao Chai, Guan hong Wang, Yucheng Zhang, Haoyang Zhou, Feiyang Wu, Haozhe Chi, Xun Guo, Tian Ye, Yanting Zhang, et al. Moviechat: From dense token to sparse memory for long video understanding. In *Proceedings of the IEEE/CVF Conference on Computer Vision and Pattern Recognition*, pages 18221–18232, 2024. 7
- [65] Sainbayar Sukhbaatar, Édouard Grave, Piotr Bojanowski, and Armand Joulin. Adaptive attention span in transformers. In *Proceedings of the 57th Annual Meeting of the Association for Computational Linguistics*, pages 331–335, 2019. 1
- [66] Hugo Touvron, Thibaut Lavril, Gautier Izacard, Xavier Martinet, Marie-Anne Lachaux, Timothée Lacroix, Baptiste Rozière, Naman Goyal, Eric Hambro, Faisal Azhar, et al. Llama: Open and efficient foundation language models. *arXiv preprint arXiv:2302.13971*, 2023. 1, 2
- [67] Peng Wang, Shuai Bai, Sinan Tan, Shijie Wang, Zhihao Fan, Jinze Bai, Keqin Chen, Xuejing Liu, Jialin Wang, Wenbin Ge, et al. Qwen2-vl: Enhancing vision-language model’s perception of the world at any resolution. *arXiv preprint arXiv:2409.12191*, 2024. 1
- [68] Zichen Wen, Yifeng Gao, Shaobo Wang, Junyuan Zhang, Qintong Zhang, Weijia Li, Conghui He, and Linfeng Zhang. Stop looking for important tokens in multimodal language models: Duplication matters more. *arXiv preprint arXiv:2502.11494*, 2025. 5, 7, 15
- [69] Long Xing, Qidong Huang, Xiaoyi Dong, Jiajie Lu, Pan Zhang, Yuhang Zang, Yuhang Cao, Conghui He, Jiaqi Wang,

- Feng Wu, et al. Pyramiddrop: Accelerating your large vision-language models via pyramid visual redundancy reduction. *arXiv preprint arXiv:2410.17247*, 2024. 5, 7, 15
- [70] Jun Xu, Tao Mei, Ting Yao, and Yong Rui. Msr-vtt: A large video description dataset for bridging video and language. In *Proceedings of the IEEE conference on computer vision and pattern recognition*, pages 5288–5296, 2016. 4, 14
- [71] An Yang, Anfeng Li, Baosong Yang, Beichen Zhang, Binyuan Hui, Bo Zheng, Bowen Yu, Chang Gao, Chengen Huang, Chenxu Lv, et al. Qwen3 technical report. *arXiv preprint arXiv:2505.09388*, 2025. 1, 2
- [72] Senqiao Yang, Yukang Chen, Zhuotao Tian, Chengyao Wang, Jingyao Li, Bei Yu, and Jiaya Jia. Visionzip: Longer is better but not necessary in vision language models. In *Proceedings of the Computer Vision and Pattern Recognition Conference*, pages 19792–19802, 2025. 5, 7, 15
- [73] Yuan Yao, Tianyu Yu, Ao Zhang, Chongyi Wang, Junbo Cui, Hongji Zhu, Tianchi Cai, Haoyu Li, Weilin Zhao, Zhihui He, et al. Minicpm-v: A gpt-4v level mllm on your phone. *arXiv preprint arXiv:2408.01800*, 2024. 1
- [74] Jiabo Ye, Anwen Hu, Haiyang Xu, Qinghao Ye, Ming Yan, Yuhao Dan, Chenlin Zhao, Guohai Xu, Chenliang Li, Junfeng Tian, et al. mplug-docowl: Modularized multimodal large language model for document understanding. *arXiv preprint arXiv:2307.02499*, 2023. 5
- [75] Xubing Ye, Yukang Gan, Xiaoke Huang, Yixiao Ge, and Yansong Tang. Voco-llama: Towards vision compression with large language models. In *Proceedings of the Computer Vision and Pattern Recognition Conference*, pages 29836–29846, 2025. 1
- [76] Weihao Yu, Zhengyuan Yang, Linjie Li, Jianfeng Wang, Kevin Lin, Zicheng Liu, Xinchao Wang, and Lijuan Wang. Mm-vet: evaluating large multimodal models for integrated capabilities. In *Proceedings of the 41st International Conference on Machine Learning*, pages 57730–57754, 2024. 4, 14
- [77] Hang Zhang, Xin Li, and Lidong Bing. Video-llama: An instruction-tuned audio-visual language model for video understanding. In *Proceedings of the 2023 Conference on Empirical Methods in Natural Language Processing: System Demonstrations*, pages 543–553, 2023. 7
- [78] Hang Zhang, Xin Li, and Lidong Bing. Video-llama: An instruction-tuned audio-visual language model for video understanding. *arXiv preprint arXiv:2306.02858*, 2023. 1
- [79] Pan Zhang, Xiaoyi Dong, Bin Wang, Yuhang Cao, Chao Xu, Linke Ouyang, Zhiyuan Zhao, Haodong Duan, Songyang Zhang, Shuangrui Ding, et al. Internlm-xcomposer: A vision-language large model for advanced text-image comprehension and composition. *arXiv preprint arXiv:2309.15112*, 2023. 2
- [80] Qizhe Zhang, Aosong Cheng, Ming Lu, Renrui Zhang, Zhiyong Zhuo, Jiajun Cao, Shaobo Guo, Qi She, and Shanghang Zhang. Beyond text-visual attention: Exploiting visual cues for effective token pruning in vlms. In *Proceedings of the IEEE/CVF International Conference on Computer Vision*, pages 20857–20867, 2025. 5, 7, 15
- [81] Qizhe Zhang, Mengzhen Liu, Lichen Li, Ming Lu, Yuan Zhang, Junwen Pan, Qi She, and Shanghang Zhang. Beyond attention or similarity: Maximizing conditional diversity for token pruning in mllms. *arXiv preprint arXiv:2506.10967*, 2025. 5, 7, 15
- [82] Renrui Zhang, Jiaming Han, Chris Liu, Peng Gao, Aojun Zhou, Xiangfei Hu, Shilin Yan, Pan Lu, Hongsheng Li, and Yu Qiao. Llama-adapter: Efficient fine-tuning of language models with zero-init attention. *arXiv preprint arXiv:2303.16199*, 2023. 7
- [83] Yuan Zhang, Chun-Kai Fan, Junpeng Ma, Wenzhao Zheng, Tao Huang, Kuan Cheng, Denis Gudovskiy, Tomoyuki Okuno, Yohei Nakata, Kurt Keutzer, et al. Sparsevlm: Visual token sparsification for efficient vision-language model inference. *arXiv preprint arXiv:2410.04417*, 2024. 5, 7, 15
- [84] Yuanhan Zhang, Jinming Wu, Wei Li, Bo Li, Zejun Ma, Ziwei Liu, and Chunyuan Li. Video instruction tuning with synthetic data. *arXiv preprint arXiv:2410.02713*, 2024. 1
- [85] Yixiao Zhou, Ziyu Zhao, Dongzhou Cheng, Zhiliang Wu, Jie Gui, Yi Yang, Fei Wu, Yu Cheng, and Hehe Fan. Dropping experts, recombining neurons: Retraining-free pruning for sparse mixture-of-experts llms. In *Findings of the Association for Computational Linguistics: EMNLP 2025*, pages 15169–15186, 2025. 1
- [86] Yixiao Zhou, Yang Li, Dongzhou Cheng, Hehe Fan, and Yu Cheng. Look inward to explore outward: Learning temperature policy from llm internal states via hierarchical rl. *arXiv preprint arXiv:2602.13035*, 2026. 2
- [87] Deyao Zhu, Jun Chen, Xiaoqian Shen, Xiang Li, and Mohamed Elhoseiny. Minigt-4: Enhancing vision-language understanding with advanced large language models. *arXiv preprint arXiv:2304.10592*, 2023. 2

Frequency-Modulated Visual Restoration for Matryoshka Large Multimodal Models

Supplementary Material

This supplementary material contains several sections that provide additional details related to our work. Specifically, it will cover the following topics:

- In Appendix A, we provide details of the experimental setup, including model architectures and evaluation benchmarks.
- In Appendix B, we provide additional experiments, including FMVR for advanced open-source LMM, FMVR for larger language model, Ablation study on other Matryoshka visual token sampling methods, and case results.

A. Details of Experimental Setup

A.1. Model Architectures

LLaVA-1.5 [45]. As a representative line of open-source multimodal large language models, the LLaVA family is widely adopted for its efficiency and strong capability. It mainly has three components, where CLIP [58] is used to extract visual representations, Vicuna [15] serves as the language backbone, and a lightweight projection module maps visual features into the LLM’s embedding space. With visual instruction tuning, this basic setup enables the model to perform a wide range of image–text tasks. LLaVA-1.5 significantly enhances multimodal reasoning ability. At the common resolution of 336×336, the model outputs 576 visual tokens for each image.

LLaVA-Next [47]. LLaVA-NeXT (also referred to as LLaVA-1.6) pushes the LLaVA architecture further by introducing a dynamic-resolution strategy aimed at strengthening the model’s visual understanding. Instead of relying on a fixed input size, it adjusts the aspect ratio according to the native dimensions of the image and allows the effective resolution to scale by up to four times. Importantly, the visual encoder itself remains unchanged. The high-resolution input is partitioned into multiple tiles, each matching the original input size, and every tile is processed independently before their visual features are concatenated and passed to the language model. This tiling-based high-resolution pipeline substantially boosts performance on tasks requiring fine-grained perception, such as OCR, detailed reasoning, and factual recognition. For consistency in our evaluations, we standardize the resolution to 672×672—four times the original—yielding a total of 2,880 visual tokens.

Qwen2.5-VL [3]. Qwen2.5-VL represents a member of

Qwen-VL family. Its visual backbone has been thoroughly redesigned, adopting a revised Vision Transformer that incorporates windowed attention, SwiGLU activations, and RMSNorm, following the architectural paradigm of the Qwen2.5 language model. Beyond static image understanding, it embraces a dynamic visual processing pipeline, supporting flexible input resolutions and adaptive frame rate handling. Thanks to these advantages, Qwen2.5-VL achieves comparable performance in detailed visual perception tasks such as detection, OCR, layout and document parsing, as well as structured information extraction.

A.2. Evaluation Benchmarks

A.2.1. General Image Benchmarks

VQA_{v2} [23]. It is the version of the VQA benchmark [2], constructed to assess a model’s integrated understanding of visual content, natural language, and commonsense reasoning. The dataset contains 265,016 images drawn from COCO [43] as well as synthetic abstract scenes, with each image paired with an average of 5.4 questions. Every question is further provided with 10 reference answers and 3 additional plausible distractor responses. Following common practice, we adopt the test-dev split for evaluation.

GQA [27]. It is a large-scale VQA dataset constructed from real-world images sourced from the Visual Genome corpus [25], aimed at evaluating the model’s capacity for compositional reasoning and fine-grained visual comprehension. It contains more than 22 million question–answer pairs, and every image is accompanied by a richly annotated scene graph that captures object categories, attributes, and inter-object relationships. For our experiments, we report results on the test-dev balanced split.

VizWiz [25]. This benchmark targets visual question answering in a real-world accessibility scenario: blind or low-vision users take photos in everyday environments and verbally pose questions about them. Each visual question is accompanied by ten answers, offering diverse perspectives on noisy and incomplete visual information. The dataset defines two core tasks—providing answers to the visual questions and detecting when a question cannot be answered from the image alone—thereby emphasizing real-world challenges such as low-quality imagery, occlusion, and ambiguous scene content. We evaluate our model on the official test split.

ScienceQA [52]. This dataset is a large-scale multimodal multiple-choice QA benchmark that covers a broad spectrum of scientific disciplines. It comprises 21,208 questions drawn from natural sciences, language sciences, and social sciences, which are further organized into 26 topics, 127 fine-grained categories, and 379 skill types. The questions vary in modality: 48.7% provide visual content, 48.2% include textual context, and 30.8% offer both forms of information. For evaluation, we follow prior works and adopt the test split that contains image-based questions (ScienceQA-IMG).

POPE [40]. This benchmark targets the evaluation of object hallucination in large vision–language models. It is constructed using images from COCO [43], enabling the measurement of hallucinated predictions. The performance is summarized using precision, recall, and F1 scores. Following prior works, we report results on the test split.

MME [9]. It evaluates both the perceptual and cognitive abilities of multimodal large language models across 14 subtasks. The perception tasks cover coarse- and fine-grained recognition as well as OCR, ranging from basic object presence, count, and attributes to identifying specific scenes, landmarks, and artworks. The cognition tasks assess commonsense reasoning, numerical calculation, translation, and code understanding.

MMBench [50]. This benchmark provides a broad evaluation of vision–language abilities across diverse tasks. It offers a larger varied set of questions and skills than prior benchmarks. MMBench also proposes a CircularEval protocol, which uses ChatGPT to convert open-ended outputs into structured choices for more stable and consistent scoring.

MM-Vet [76]. It examines the integration of multiple multimodal abilities. It covers six core capabilities—recognition, OCR, knowledge, language generation, spatial reasoning, and mathematics—through 218 challenging examples. Evaluation is conducted using a ChatGPT-based assessor, which provides unified metrics for answers of different formats.

A.2.2. Text-oriented benchmarks

TextVQA [62]. This benchmark examines the model’s capacity to recognize and reason over textual content embedded in images. The visual data, largely drawn from Open Images v3 [33], contains real-world settings such as signs, advertisements, and product labels, all featuring substantial scene text. As a result, the benchmark provides an assessment of OCR integration and text-sensitive visual reasoning. We evaluate on the validation split.

ChartQA [55]. It is a large benchmark for chart-based question answering, emphasizing visual understanding and logical or complex reasoning. It contains 9.6K human-written questions and 23.1K questions generated from chart summaries. Unlike earlier template-driven datasets,

Table 8. Performance comparison of different pruning methods on Qwen2.5-VL-7B.

Methods	#Vision Tokens	TextVQA	ChartQA	AI2D	MMB ^{EN}	Avg. (%)
Qwen2.5-VL	1296	84.8	86.1	80.4	82.8	83.5
FastV	128	73.8	52.2	71.4	72.9	67.6
DivPrune	128	67.0	50.4	72.1	77.8	66.8
CDPruner	128	77.8	59.2	74.0	76.2	71.8
FMVR (Ours)	81	76.3	62.2	77.5	79.6	73.9

ChartQA requires multi-step reasoning over both chart visuals and their underlying data. We use the test split for evaluation.

AI2D [31]. AI2D is a diagram-based question answering benchmark containing over 5,000 grade-school science diagrams, annotated with more than 150,000 structured labels and syntactic parses. It also provides over 15,000 multiple-choice questions paired with the diagrams, supporting research on visual reasoning and scientific diagram understanding. We use the masked test split for evaluation.

A.2.3. Video benchmarks

MSVD [10]. MSVD is a video question answering benchmark, containing roughly 2k short video clips and about 50k question–answer pairs. It evaluates a model’s ability to understand visual content over time, including actions, events, and temporal relationships, as well as its capacity to ground and answer natural language queries about the video.

MSRVTT [70]. It is a large-scale video captioning and video understanding dataset consisting of 10k video clips collected from real-world web videos. Each video is paired with 20 captions, covering a broad range of everyday events, activities, and scenes. The dataset is widely used for video–language tasks such as video captioning, video retrieval, and video question answering, serving as a standard benchmark for evaluating multimodal temporal understanding.

ActivityNet [5]. It is a large-scale benchmark for human activity understanding in untrimmed videos. It contains around 20k videos spanning 200 activity categories, covering a wide range of daily human actions. Designed for tasks such as action recognition, temporal action localization, and temporal segmentation, ActivityNet provides diverse and long-duration videos that evaluate both visual perception and temporal reasoning capabilities of multimodal models.

Video-based Generative Performance Benchmark [54]. It contains five dimensions: correctness, detail orientation, contextual understanding, temporal understanding, and consistency. The evaluation pipelines for both the open-ended question-answering and the generative performance benchmarks adhere to Video ChatGPT [54].

Table 9. Performance comparison on LLaVA-1.5-13B across 10 image-based benchmarks. ‘#VisionTokens’ is the number of vision tokens. Δ rows show the change vs. LLaVA-v1.5-13B.

Methods	#Vision Tokens	VQAv2	GQA	VisWiz	SQA ^{IMG}	VQA ^{Text}	POPE	MME	MMB ^{EN}	MMB ^{CN}	MMVet	Avg. (%)
LLaVA-1.5-13B [45]	576	80.0	63.3	53.6	72.8	61.2	86.0	1531.2	68.5	63.5	36.2	66.2
FastV [12]	128	75.3	58.3	54.6	74.2	58.6	75.5	1460.6	66.1	62.3	32.8	63.1
PyramidDrop [69]	128	78.2	61.0	53.8	73.3	60.2	83.6	1489.5	67.5	62.8	32.1	64.7
SparseVLM [83]	128	77.6	59.6	51.4	74.3	59.3	85.0	1487.9	68.4	62.6	35.2	64.8
Prumerge+ [60]	128	76.2	58.3	52.8	73.3	56.1	82.7	1445.9	66.3	61.2	33.6	63.3
TRIM [63]	128	76.4	59.4	49.7	72.4	55.0	86.8	1426.9	67.1	58.4	35.1	63.2
VisionZip [72]	128	76.8	57.9	52.3	73.8	58.9	82.7	1449.2	67.4	62.5	36.0	64.1
DART [68]	128	75.7	57.7	53.0	74.2	58.7	80.4	1395.0	65.4	62.2	34.8	63.2
DivPrune [1]	128	77.1	59.2	53.5	72.8	58.0	86.8	1457.7	66.3	60.7	34.4	64.2
CDPruner [81]	128	77.7	59.7	52.9	73.2	58.4	87.3	1478.0	67.5	61.5	36.2	64.8
VisPruner [80]	128	76.1	58.8	53.4	72.8	57.9	86.0	1452.2	66.4	61.3	36.1	64.1
MQT-LLaVA [26]	144	77.9	59.4	54.1	73.6	60.2	86.1	1471.3	66.5	61.0	31.4	64.4
M3 [6]	144	79.2	60.6	53.5	72.9	60.4	87.7	1478.3	67.2	59.8	32.3	64.8
Ours												
	1	72.2	57.6	50.3	69.4	53.9	82.5	1384.7	62.2	55.8	27.8	60.1
	9	76.3	60.2	51.8	70.9	58.4	84.7	1470.5	65.1	60.4	30.7	63.2
FMVR-LLaVA	36	78.4	61.2	53.4	71.5	60.5	86.6	1477.8	66.3	62.5	32.7	64.7
	144	79.7	63.6	56.7	72.0	61.3	87.2	1489.4	68.3	63.8	34.2	66.1
	576	80.7	64.2	57.2	72.4	60.7	88.1	1528.9	69.5	65.1	35.4	67.0
Δ vs. LLaVA-v1.5-13B	144	-0.3	+0.3	+3.1	-0.8	+0.1	+1.2	-41.8	-0.2	+0.3	-2.0	-0.1

Table 10. Ablation study on Matryoshka visual token sampling, including average pooling, sequential sampling, spatial sampling, and max pooling.

Num of Vis Tokens	TextVQA				MMBench			
	Avg Pooling	Sequential	Spatial	Max Pooling	Avg Pooling	Sequential	Spatial	Max Pooling
1	49.2	46.3	45.9	47.1	60.7	57.9	58.6	59.8
9	50.8	46.7	46.4	48.2	64.2	60.4	61.5	63.9
36	55.3	51.2	49.0	52.8	65.2	61.8	63.1	64.5
144	55.5	53.7	50.6	53.3	65.8	64.2	63.7	64.9
576	57.8	55.6	52.6	54.7	65.9	64.7	64.0	65.3

B. Additional Experimental Results

B.1. FMVR for advanced open-source LMM

In addition to LLaVA, we further apply FMVR to one of the most advanced open-source LMM, i.e., Qwen2.5-VL. The input image is resized to 1008×1008 and the visual encoder produces a total of 1,296 tokens. We directly insert the trained FMVR into the back of the Qwen2.5-VL’s visual encoder. We compare our FMVR with FastV DivPrune, and CDPruner. As shown in Table 8, FMVR consistently achieves the best results across on four benchmarks. FMVR with 81 visual tokens outperforms the next-best method, CDPruner with 128 visual tokens, by 2.1% in average. It demonstrates the strong generalizability of FMVR on advanced LLM architectures.

B.2. FMVR for larger language model

To further examine whether our approach scales to stronger language backbones, we conduct experiments on LLaVA-1.5-13B. As shown in Table 9, Increasing the size of LLM yields substantial performance gains. Across all token pruning methods with 128 visual tokens except for SparseVLM, CDPruner, and M3, FMVR with only 36 visual tokens consistently achieves the highest performance 64.7%. It is worth noting that our FMVR with 144 visual tokens achieved comparable performance to LLaVA-1.5-13B with 576 visual tokens, i.e., 66.1% vs. 66.2%, demonstrating its effectiveness on larger language models.

Table 11. Baseline results of token numbers on LLaVA-1.5-7B.

Tokens	Method	VQAv2	GQA	VisWiz	SQA ^{IMG}	VQA ^{Text}	POPE	MME	MMB ^{EN}	MMB ^{CN}	MMVet
576	baseline	78.5	62.0	50.0	66.8	58.2	85.9	1510.7	64.3	58.3	30.5
	Ours	79.2	63.0	56.5	68.9	57.8	87.5	1510.1	65.9	58.0	34.3
144	baseline	77.8	61.1	48.3	67.5	57.3	85.0	1480.4	65.1	57.1	30.2
	Ours	78.6	62.3	55.1	69.7	55.5	86.4	1473.9	65.8	57.6	33.4
36	baseline	76.1	58.4	46.8	67.0	56.7	85.2	1448.3	64.5	57.7	29.4
	Ours	76.5	60.9	52.9	69.5	55.3	85.9	1452.5	65.2	58.3	32.2
9	baseline	73.4	56.3	46.0	67.3	52.2	83.6	1422.9	63.7	56.8	28.5
	Ours	74.5	59.1	50.7	69.9	50.8	84.1	1415.0	64.2	57.5	29.0
1	baseline	67.4	54.2	45.5	66.4	49.6	79.5	1291.0	58.2	53.9	26.2
	Ours	68.3	55.2	49.7	68.6	49.2	81.1	1284.8	60.7	53.4	26.4

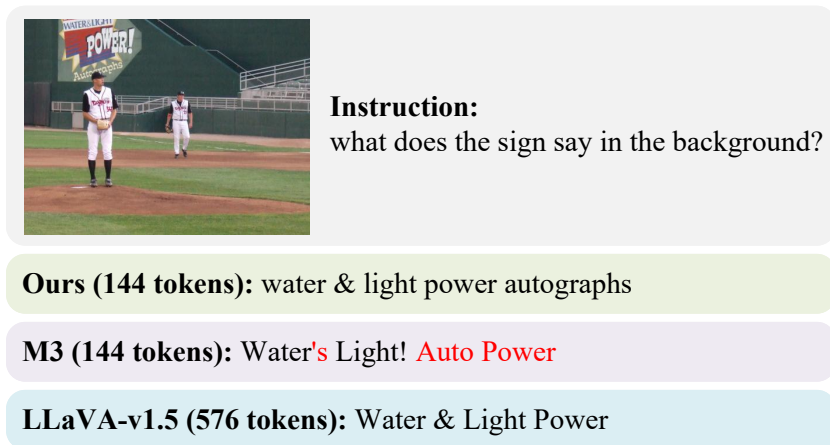


Figure 7. Example demonstrating FMVR’s image understanding capability on more challenging OCR task. Response marked in red indicates errors.

B.3. Ablation study on other Matryoshka visual token sampling methods

We evaluate four strategies for selecting visual tokens in Matryoshka visual token construction, including average pooling, spatial sampling, sequential sampling, and max pooling. As illustrated in Table 10, average pooling consistently outperforms the other three approaches because it preserves the complete local semantic information by aggregating all tokens within each spatial region. In contrast, spatial sampling and sequential sampling select only one token from each region or sequence, which discards important information and disrupts spatial consistency. Max pooling keeps only the strongest activation, ignoring other semantic information. As a result, average pooling provides the most informative representation, leading to superior performance.

B.4. Additional case results

Fig. 7 presents an example that highlights FMVR’s strength on a challenging OCR task. The text in the image varies in

size and is somewhat obscured, which typically degrades recognition performance in LLMs. Despite this difficulty, our FMVR correctly read all the text using only 144 visual tokens. In contrast, M3 misidentify key words, such as mistakenly identifying ‘autographs’ as ‘auto power’ and introduce an incorrect ‘s’. Furthermore, LLaVA-v1.5 fails to recognize ‘autographs’. These results demonstrate that FMVR possesses more detailed visual perception capabilities.

B.5. Baseline results of token numbers

Table 11 reports the baseline and our method under different token budgets on LLaVA-1.5-7B. As token numbers decrease from 576 to 1, performance gradually drops. However, our method consistently outperforms the baseline on most benchmarks, demonstrating stronger robustness and effectiveness under aggressive token reduction.